Solution Structure of the DNA Damage Lesion 8-Oxoguanosine from Ultraviolet Resonance Raman Spectroscopy

Namrata Jayanth, Srinivas Ramachandran, and Mrinalini Puranik*

National Centre for Biological Sciences, TIFR, GKVK Campus, Bellary Road, Bangalore 560065, India

Received: August 11, 2008; Revised Manuscript Received: December 9, 2008

UV radiation and reactive byproducts of cellular metabolism are constant threats to genomic stability. A frequent consequence is the oxidation of DNA nucleobases, especially guanine to 8-oxoguanosine. This highly mutagenic lesion can form base pairs with other nucleobases, does not significantly distort the DNA structure, and remains unnoticed by DNA polymerases. Detection and biophysical studies of modified nucleobases is challenging because they are not fluorescent and have broad electronic spectra that overlap with those of normal bases. The structure of 8-oxoguanosine and its anion in solution has been contentious in the literature. Using ultraviolet excitation in resonance with the nucleobase, we have obtained the Raman spectra of 8-oxoguanosine. The stable tautomer in solution is unequivocally identified as the diketone form. We show that, at high pH, 8-oxoguanosine gets deprotonated to form an anion through loss of the N1 proton from the pyrimidine ring. The enol form is never populated to a detectable level. Raman spectra are supported by density functional theoretical calculations and a complete normal-mode analysis to identify bands that can be used as reporters of protein−nucleobase interactions. We have demonstrated that UVRR spectra provide unprecedented information on the solution-state structures of modified nucleobases.

Introduction

Structural integrity of cellular DNA is endangered by multiple external and internal damage agents such as UV and other ionizing radiation, drugs, and reactive oxygen species. Action of these damage agents on DNA results in strand breaks, cross-linking of nucleobases,[1] and base oxidation.[2] The presence of modified nucleobases (called lesions) in DNA can cause mutagenesis, and in large quantities, such lesions can be lethal to cells. The importance of such single-base modifications is corroborated by the existence of a highly efficient, dedicated repair pathway in both eukaryotes and prokaryotes called base excision repair (BER). It is estimated that the BER pathway is involved in the repair of 20000 lesions per cell per day.[3] BER involves specific recognition of the modified nucleobase, followed by expulsion and excision of the base via hydrolysis of the glycosidic bond by enzymes called DNA glycosylases. Over 100 DNA lesions have been identified, and several groups around the world have isolated and purified the more abundant of these.[4,5] 8-Oxoguanine and the corresponding nucleoside and nucleotide have been extensively investigated as markers of oxidative damage in several systems for their mutagenic potential. Recently, Nakabeppu and co-workers studied the genome-wide distribution of 8-oxoguanosine with fluorescent in situ detection on human metaphase chromosomes and found that it correlates with the regions for recombination and single-nucleotide polymorphisms.[6]

Although undesirable in the cellular context, there is an increasing interest in using modified nucleobases in making novel nucleic-acid-based nanostructures, e.g., the use of 8-oxoguanosine in G-quadruplexes for their altered hydrogen-bonding properties. Knowledge of the precise protonation and tautomeric states in solution at a given pH is indispensable in the design of novel DNA nanostructures. The results reported in this article unequivocally establish the solution structure of 8-oxoguanosine at different pH values and demonstrate a novel application of modified nucleobases as site-specific spectroscopic labels in nucleic acids.

Of the four bases, guanine is most susceptible to damage because of its low ionization potential ($IP_G = 7.51$ eV).[7] The ionization potential is further reduced (to $IP_{GG} = 7.28$ eV) in the proximity of a neighboring guanosine nucleobase in a DNA strand. Oxidation of guanosine can lead to the formation of products such as formamidopyrimidine, a form in which the imidazole ring opens, or a modified purine called 8-oxoguanosine by addition of oxygen to the C8 carbon of the imidazole ring (Figure 1). The latter lesion, 8-oxoguanosine (8OG), is formed in higher quantum yield than other guanine lesions.[8,9] The presence of 8-oxoguanosine in a DNA strand does not lead to a significant distortion of the DNA structure, as 8-oxoguanosine can form hydrogen-bonded pairs with other nucleobases. During replication, the presence of 8-oxoguanosine leads to G:C to T:A transversion mutations that result from 8OG:A mispairing during replication.[10,11]

The effects of substitution at the N7 and C8 positions on the structure of guanosine are subtle. 8-Oxoguanosine in DNA forms normal Watson−Crick base pairs with both cytosine and adenine.[12] Consequently, the mechanism by which DNA repair enzymes such as formamidopyrimidine glycosylase (FPG/MutM) and human OGG1 enzyme (hOGG1) differentiate between 8-oxoguanosine and the normal nucleoside guanosine is intriguing. Fundamental to this question is an understanding of the detailed structure and charge distribution of 8-oxoguanosine and its various protonation states, especially the 8-oxoguanosine anion, vis-à-vis normal guanosine and its corresponding protonation states.

The structure, pH dependence, and base-pairing properties of 8-oxoguanosine in solution, as a free base and when incorporated into a DNA oligomer, have been extensively studied using various techniques. NMR studies on the tautom-

* To whom correspondence should be addressed. Phone: +91-80-23666160. Fax: +91-80-23636662. E-mail: mpuranik@ncbs.res.in.

10.1021/jp8071519 CCC: $40.75
Published on Web 02/03/2009

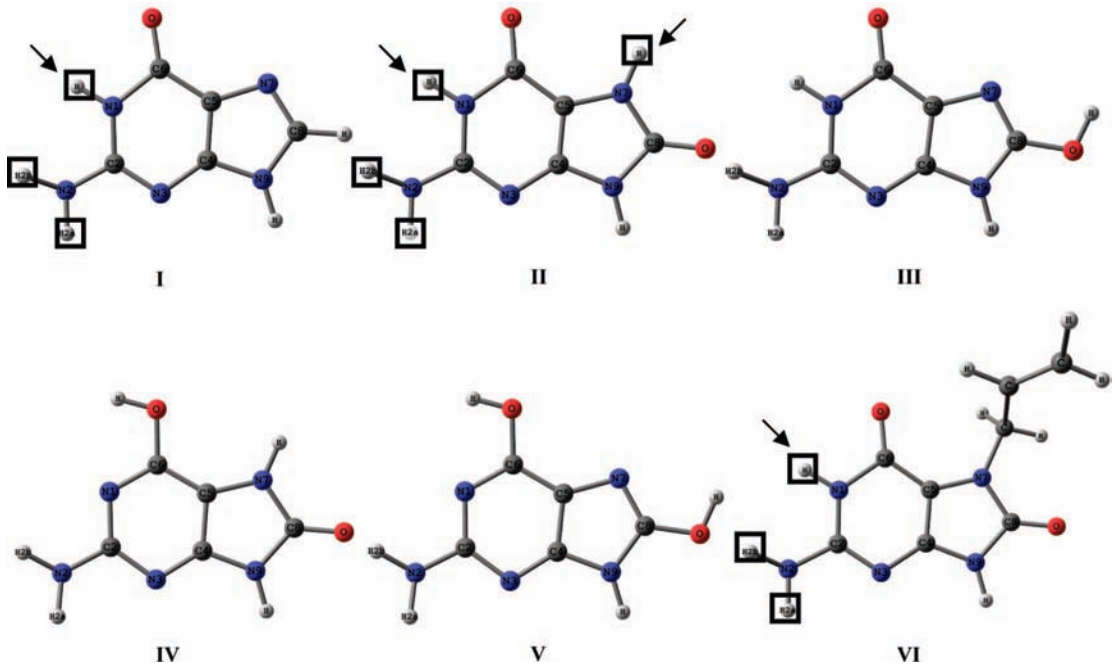

Figure 1. Structure and numbering used in calculations for (I) guanine, (II) 6,8-diketoguanine, (III) 6-keto-8-enolguanine, (IV) 6-enol-8-ketoguanine, (V) 6,8-dienolguanine, and (VI) 7-allyl-8-oxoguanine. The possible deprotonation sites for formation of monoanions of (I) guanine, (II) 6,8-diketoguanine, and (VI) 7-allyl-8-oxoguanine are indicated with arrows. Hydrogen atoms expected to exchange with deuterium in experiments involving solutions of GMP, 8-oxoguanosine, and 7-allyl-8-oxoguanosine in D_2O are marked with squares. Isotopic shifts in the vibrational spectra were computed by replacing the indicated hydrogen atoms (indicated with squares) with deuterium. Figures were made using Chemcraft 1.5 from the geometry computed using GAMESS. The H2b—N2—C2—N3 dihedral angles in the structures of (I) guanine and (II) 6,8-diketoguanine are 148.1° and 148.8°, respectively.

erism of this molecule using ^{15}N and ^{13}C isotopic labeling showed that the predominant form of 8-oxoguanosine in solution is the 6,8-diketone form at neutral pH.[13] NMR spectroscopy has also been used to observe the effect of the presence of 8-oxoguanosine on the structure of DNA duplex. 8-Oxoguanosine within DNA is also in the 6,8-diketo form and makes Watson—Crick-type hydrogen bonds when base-paired with cytosine.[12,14] Ab initio calculations of gas-phase and aqueous 8-oxoguanosine support findings of the NMR experiments at neutral pH.[1,15,16] The identity of the predominant tautomer of the nucleoside 8-oxoguanosine at elevated pH has been contentious in the literature. NMR experiments suggested that 8-oxoguanosine converts to the monoenol form at high pH.[17,18]

The UV—vis absorption spectra of guanosine and 8-oxoguanosine in solution are broad, with overlapping bands. Resonance Raman spectra, on the other hand, are highly sensitive to subtle changes in the structure and environment of a molecule and are expected to be different for guanosine and 8-oxoguanosine. Direct detection of the neutral form of 8-oxoguanosine with Raman spectroscopy was reported by Kundu and Loppnow.[19] They noted that the Raman spectrum of 8-oxoguanosine is indeed different from that of guanosine and reported a preliminary assignment.

Herein, we report high-resolution ultraviolet resonance Raman vibrational spectra of 8-oxodeoxyguanosine; its 7-allyl-substituted analogue, 7-allyl-8-oxoguanosine; and their anionic forms at high pH using 260-nm Raman excitation. Spectra of H/D-exchanged molecules were also obtained to aid assignment. The structures and vibrational spectra of the nucleobases, 8-oxoguanine, its tautomeric and protonation states, 7-allyl-8-oxoguanine, and guanine computed using density functional theory (DFT) methods with a high-level basis set (6-31G**) are reported and compared with experimental vibrational spectra. The reliability of computational predictions was tested by isotopic labeling with deuterium in both experiments and theoretical studies. Our results demonstrate that ultraviolet resonance Raman (UVRR) spectroscopy provides a novel and sensitive method to elucidate structural changes in guanine upon oxidation. The unique RR spectrum of 8-oxoguanosine allows the observation of 8-oxoguanosine in the presence of guanine and other nucleobases in studies involving DNA oligomers. Using UVRR and FTIR spectroscopies and computational modeling of 8-oxoguanosine and the judiciously chosen model compound 7-allyl-8-oxoguanosine, we established the solution structures of 8-oxoguanosine and its anion with certainty.

The structure of the anionic form is of direct relevance to understanding the mechanism of recognition and catalysis of this substrate by DNA repair enzymes, which are predicted to proceed via S_N1 and S_N2 mechanisms. From these analyses, we predict the normal modes that can be used as reporters of the interaction of the nucleobase with protein active sites.

The experimental studies reported here were done on 8-oxo-2′-deoxyguanosine (8-oxodG), 7-allyl-8-oxoguanosine (7AOG), and guanosine-5′-monophosphate (GMP) disodium salt, whereas the computational studies were carried out on the corresponding nucleobases 8-oxoguanine, its tautomers and protonation states, and guanine. We refer to the molecules as 8-oxoguanosine, 7-allyl-8-oxoguanosine, and GMP, where both experimental and computational results are discussed in the article for convenience.

Experimental and Computational Methods

Sample Preparation. 8-Oxo-2′-deoxy-guanosine, 7-allyl-8-oxoguanosine, and guanosine-5′-monophosphate disodium salt (Sigma-Aldrich, St. Louis, MO) were of highest purity available and of HPLC grade and were used without further purification. Samples for Raman experiments were 0.5 mM in concentration and were prepared by dissolving appropriate quantities of the

corresponding purines in 18 MΩ purity water (Millipore) or D_2O (Sigma-Aldrich, St. Louis, MO). Samples were dissolved in D_2O and left overnight before their spectra were recorded to ensure complete H/D exchange. The pH of the samples was adjusted by the addition of appropriate amounts of 10 M sodium hydroxide (NaOD for samples in D_2O). Acetonitrile, trichloroethylene, isopropanol, indene, and cyclohexane used for calibration were HPLC grade, were purchased from Ranchem Chemicals (Shanghai, China) or Sigma-Aldrich, and were used without further purification. HPLC-purified oligonucleotides were purchased from Midland Certified Reagent Company (Midland, TX). The oligonucleotides used were 5′-CTCTCTCGGCCTTCC-3′ and 5′-CTCTCTC(8-oxoguanosine)GCCTTCC-3′. The oligonucleotides were dissolved in 18 MΩ purity water (Millipore) to a concentration of 0.5 mM for Raman experiments.

UV−Visible Absorption and FTIR Spectra. Ultraviolet spectra were recorded with an Ultraspec 4000 UV/visible spectrophotometer from Pharmacia Biotech. Infrared spectra were recorded on an IFS 66 V/S instrument (Bruker), and the samples were prepared as KBr pellets (10 μg of sample/100 μg of KBr).

Ultraviolet Resonance Raman Spectroscopy. Resonance Raman spectra were obtained by excitation with 260-nm light that was generated as follows: The frequency-doubled output of a nanosecond-pulsed Nd:YLF laser (Evolution, Coherent Inc.) at 527 nm (1-kHz repetition rate) was used to pump a Ti−S laser (Indigo, Coherent Inc.) that, in turn, generated output light of infrared wavelength. The output light of the Ti−S laser was doubled using a BBO crystal to obtain light of visible wavelength. The visible and IR outputs were mixed in another BBO crystal to generate the third-harmonic UV light at 260 nm. The typical average power at the sample was less than ∼600 μW. Samples were illuminated using a 135° backscattering geometry to minimize reabsorption by the sample, and the tube was spun about its axis to minimize damage. The scattered light was collected and focused using a pair of fused-silica lenses into a monochromator (Jobin-Yvon) that was equipped with a single, 3600 groove/mm grating for dispersing the light. Spectra were recorded with a 1024 × 256 pixel, back-illuminated CCD camera (Jobin-Yvon) and calibrated using known solvent bands. The solvents used were dimethyl formamide, acetonitrile, trichloroethylene, isopropanol, indene, and cyclohexane, all of HPLC grade, from Ranchem Chemicals and Sigma, and they were used without further purification. In experiments where the relative shift was measured, the spectra were recorded without changing the spectrometer position and are accurate to ±3 cm^{-1}. All spectral processing was carried out using the software Synergy (Jobin-Yvon). Band positions were determined by fitting Lorentzian line shapes to the bands in the observed spectra.

Computational Methods. Calculations were done on the nucleobases corresponding to the nucleosides and nucleotides used in experiments; the sugar and phosphate groups were not included in the calculations. Because the Raman excitation wavelength used was in resonance with the nucleobase, the vibrational spectrum was dominated by vibrational bands from the nucleobases, with a minor contribution from the ribose and none from the phosphate group. Hence, the vibrational spectra of the nucleobase provide a good prediction of the observed spectrum. Density functional theoretical calculations were performed with the GAMESS suite of programs[20] using the B3LYP parametrization.[21,22] The basis set used was 6-31G**, which has additional polarization functions on the hydrogens. Frequencies were computed at the optimized geometry within the harmonic approximation using GAMESS. Mulliken charges as computed in GAMESS were used for charge analysis. The possible protonation and deprotonation sites for 8-oxoguanine are shown in Figure 1.

The potential energy distributions (PEDs) were obtained using the Vibrational Energy Distribution Analysis VEDA 4.0 program.[23] The input file for VEDA was generated using the Cartesian coordinates and force-constant matrix computed with the GAMESS program. The structures of the energy-minimized molecules and normal modes of vibration were visualized using Chemcraft (http://www.chemcraftprog.com).

Results and Discussion

Structure and Charge Distribution of 8-Oxoguanine in the Gas Phase, in DNA, and in Protein-Bound Form. The structures of guanine and the four possible tautomers of 8-oxoguanine computed using DFT (B3LYP/6-31G**) are shown in Figure 1, and the structural parameters for the 8-oxoguanine and 8-hydroxyguanine (8OHG) molecules are listed in Table 1. The structures of guanine in the gas phase and in solution have been reported by several groups.[24−26] A thorough computational study of the guanine structure and vibrational spectra was reported by Giese and McNaughton.[27] High-level calculations have shown that the NH_2 group is bent out of the plane of the purine ring and that additional polarization functions are required in the basis set to determine the correct structure.[28−30] This out-of-plane distortion is attributed to two distinct effects, the partial sp^3 hybridization of the amino group and the repulsion of one of the hydrogens of the NH_2 group with the hydrogen atom at N1.[31] Therefore, we used a nonplanar starting geometry and the 6-31G** basis set with additional functions on hydrogens to determine the structures of 8-oxoguanine and its tautomers to allow a full optimization. The NH_2 group is distorted out of the plane of the purine ring in 8-oxoguanine as in guanine.[32]

Replacement of the C8−H group by a carbonyl to form the diketone structure (C8−H → C8=O) is expected to primarily affect the electron distribution in the imidazole ring. This prediction is borne out by the computed geometrical parameters in Table 1. The C8−N7 double bond in guanine (1.308 Å) changes to a single bond in 8-oxoguanine and is correspondingly longer at 1.389 Å. The C8−N9 bond is elongated by ∼0.03 Å, a much smaller effect, and the C4−C5 bond in the 8-oxoguanine molecule is shorter by a similar amount. Whereas the C6=O bond is marginally longer in 8-oxoguanine as compared to that in guanine, the C8=O bond is predicted to be of similar length to the C6=O in guanine. The computed geometry of 8-hydroxyguanine is closer to that of the natural nucleobase guanine rather than 8-oxoguanine. The C6=O bond, however, is predicted to be slightly longer in the 8-hydroxyguanine molecule than in guanine.

The crystal structure of a DNA dodecamer containing 8-oxoguanine was solved by Lipscomb and co-workers.[33] The 8-oxoguanine bound forms of hOGG1[34] and *Bacillus stearothermophilus* MutM/FPG have been reported by Fromme and Verdine.[35] Parameters of 8-oxoguanine extracted from these published structures are compared with the current calculations in Table 1. The computed structure corresponds to a molecule in the gas phase and is expected to differ from that observed in the crystal. Additionally, the structure observed in the crystal is influenced by the incorporation of 8-oxoguanine base into either the DNA helix or the protein active site.

The structure of the 8-oxoguanine anion formed by deprotonation at N1 was computed, and the structural parameters are

TABLE 1: Geometrical Parameters[a] of Guanine, 8-Oxoguanine, 8-Oxoguanine Anion, and 8-Hydroxyguanine[b] Computed Using Density Functional Theory[c] and Experimental Data Taken from Crystal Structures

geometry	guanine DFT	guanine in DNA, X-ray structure[33]	8-oxoguanine DFT	8-oxoguanine in DNA, X-ray structure[33]	8-oxoguanine with *B.st*[d] FPG, X-ray structure[35]	8-oxoguanine anion[e] DFT	8-hydroxyguanine DFT
N_1C_2	1.371	1.398	1.369	1.339	1.40	1.330	1.370
C_2N_3	1.313	1.335	1.315	1.344	1.34	1.355	1.313
N_3C_4	1.358	1.363	1.355	1.364	1.37	1.343	1.357
C_4C_5	1.396	1.367	1.382	1.358	1.39	1.376	1.392
C_5C_6	1.442	1.432	1.421	1.443	1.42	1.438	1.436
C_6N_1	1.440	1.380	1.436	1.370	1.40	1.397	1.441
C_4N_9	1.370	1.354	1.375	1.345	1.38	1.398	1.381
N_9C_8	1.384	1.376	1.412	1.395	1.37	1.400	1.377
C_8N_7	1.308	1.287	1.389	1.340	1.29	1.378	1.302
N_7C_5	1.383	1.374	1.395	1.383	1.38	1.409	1.391
C_2N_2	1.377	1.334	1.375	1.294	1.34	1.413	1.379
N_2H_{2a}	1.011	–	1.011	–	–	1.013	1.011
N_2H_{2b}	1.011	–	1.010	–	–	1.013	1.011
N_1H_1	1.013	–	1.014	–	–	–	1.013
N_9H	1.009	–	1.008	–	–	1.006	1.009
N_7H	–	–	1.007	–	–	1.006	–
C_8H	1.082	–	–	–	–	–	–
C_6O	1.218	1.220	1.225	1.217	1.24	1.247	1.220
C_8O	–	–	1.217	1.244	1.22	1.234	1.344
O_8H	–	–	–	–	–	–	0.970

[a] Distances given in angstroms. [b] See Figure 1 for atom numbering. [c] Bond lengths calculated using the B3LYP/6-31G** level of theory. [d] *Bacillus stearothermophilus*. [e] Deprotonated at N1.

listed in Table 1. The structure of the anion formed by deprotonation at N7 was also computed (not shown because experimental data confirm that the H1 proton is removed, vide infra). The N1—C2 and the N1—C6 bonds are shortened as a consequence of deprotonation at N1. Both the carbonyl bonds are lengthened, with a larger effect on C6═O than on C8═O, which can be explained by the proximity of the former.

Table S1 of the Supporting Information lists the Mulliken charge analyses of guanine, 8-oxoguanine, and 8-hydroxyguanine. Consistent with the predicted geometry, the primary differences are in the imidazole ring. The negative change on N7 is higher in both 8-oxoguanine and 8-hydoxyguanine than in guanine. The positive charge on the C8 atom increases correspondingly in 8-oxoguanine to 0.75 compared to guanine (0.27). The negative charge on O8 is similar in magnitude to the charge on O6.

Effect of Oxidation on the Electronic Structure of Guanosine. The absorption spectra of GMP and 8-oxoguanosine are distinct, as expected, with the overall redistribution of electron density in the imidazole ring due to the presence of a second carbonyl group (Figure 2). GMP has a broad absorption band with λ_{max} at 251 nm, a shoulder at 275 nm, and an intense absorption at 200 nm that is assigned to the $\pi-\pi^*$ transition of the base. The 8-oxoguanosine spectrum, on the other hand, has two lower-energy absorption maxima at 246 and 294 nm, in addition to the higher-intensity absorption at 205 nm. The reorganization of the electronic density in the purine ring following the introduction of a carbonyl group is expected to significantly perturb the molecular orbital compositions and energy gaps. Figure 3 shows the computed molecular orbitals of 8-oxoguanine and guanine. Whereas the highest occupied molecular orbital (HOMO) of guanine is essentially a π orbital on the imidazole ring with a small amount of electron density on the O6 atom, the corresponding orbital of 8-oxoguanine is delocalized to the C8═O group in addition to the C6═O group. The lowest unoccupied molecular orbitals (LUMOs) of guanine and 8-oxoguanine are similar, with the main contribution to the electron density being from the pyrimidine ring.

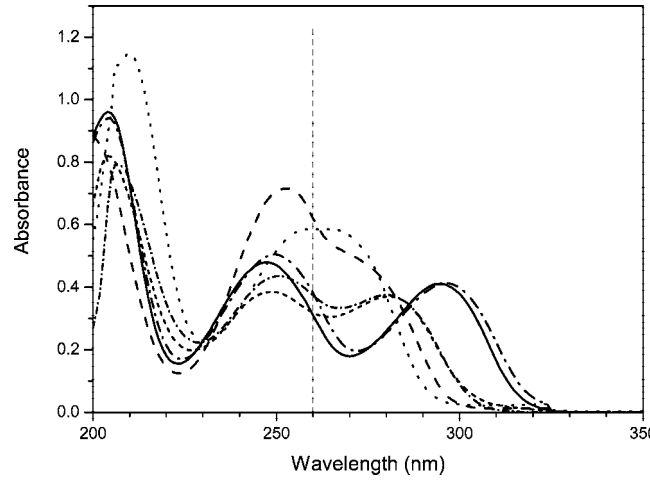

Figure 2. UV absorption spectra of aqueous solutions (50 μM) of 8-oxoguanosine at pH 7.0 (solid line), 8-oxoguanosine at pH 9.5 (short dashed line), 7-allyl-8-oxoguanosine at pH 7.0 (dash-dotted line), 7-allyl-8-oxoguanosine at pH 11.0 (short dash-dotted line), GMP at pH 7.0 (dashed line), and GMP at pH 10.5 (dotted line).

Ultraviolet Resonance Raman Spectra of 8-Oxoguanosine and 7-Allyl-8-oxoguanosine in Water and D_2O Reveal the Presence of a Single Diketone Tautomer. The spectra of 8-oxoguanosine, 7-allyl-8-oxoguanosine, and GMP in water recorded with 260-nm excitation are shown in Figure 4 (high-Raman-shift region) and Figure 5 (low-Raman-shift region). This wavelength of excitation is in resonance with the absorption of the nucleobases; hence, the vibrational bands corresponding to the nucleobase are expected to be enhanced, and the vibrations from the ribose and phosphate moieties are expected to be weak. The vibrational spectra of the corresponding nucleobases, 8-oxoguanine and guanine, were also computed using density functional theoretical methods employing the B3LYP hybrid functional with a 6-31G** basis set. Only the nucleobases corresponding to the nucleosides and nucleotides used in experiments were modeled because the experimental vibrational spectrum is dominated by the nucleobase vibrations. The

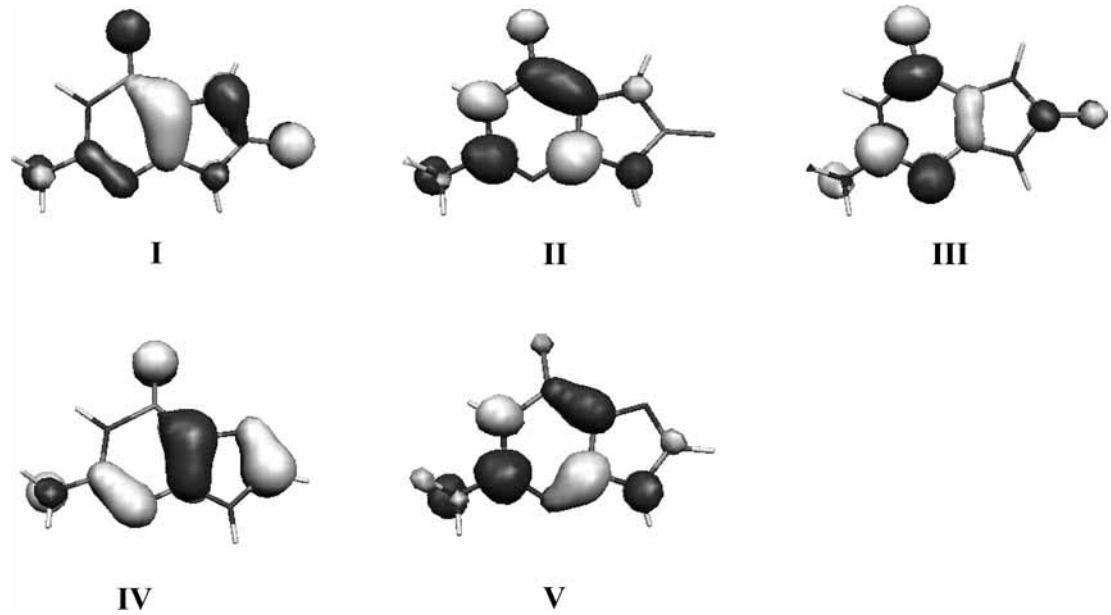

Figure 3. Computed molecular orbitals of 8-oxoguanine and guanine: (I) HOMO, (II) LUMO, (III) LUMO + 1 of 8-oxoguanine, (IV) HOMO of guanine, and (V) LUMO of guanine.

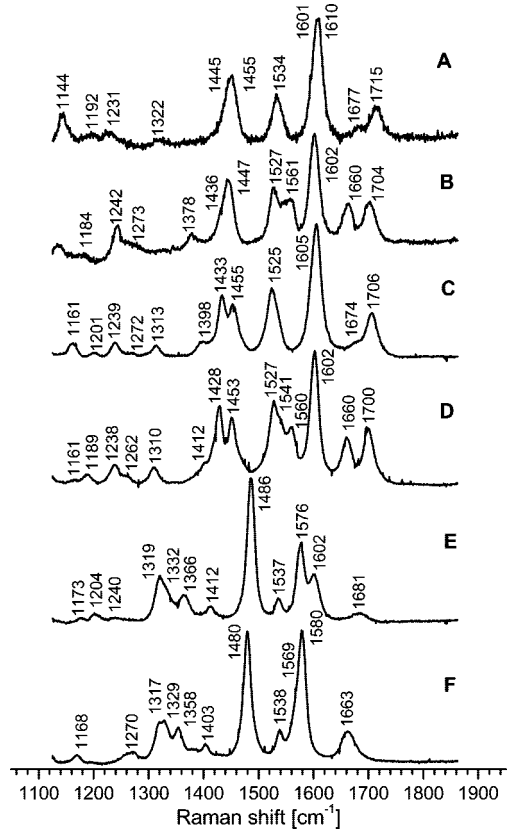

Figure 4. UVRR spectra of (A) 8-oxoguanosine in water, (B) 8-oxoguanosine in D_2O, (C) 7-allyl-8-oxoguanosine in water, (D) 7-allyl-8-oxoguanosine in D_2O, (E) GMP in water, and (F) GMP in D_2O in the high-Raman-shift region obtained with excitation at 260 nm.

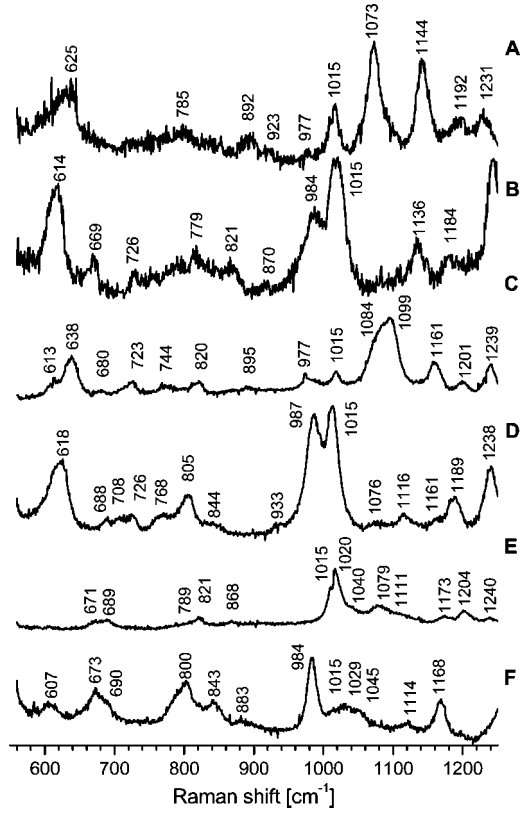

Figure 5. UVRR spectra of (A) 8-oxoguanosine in water, (B) 8-oxoguanosine in D_2O, (C) 7-allyl-8-oxoguanosine in water, (D) 7-allyl-8-oxoguanosine in D_2O, (E) GMP in water, and (F) GMP in D_2O in the low-Raman-shift region with excitation at 260nm.

computed vibrational shifts and their mode descriptions with potential energy distributions are listed in Table 2, along with the experimental Raman and infrared vibrational shifts. There are four possible tautomeric forms of 8-oxoguanosine in solution, as shown in Figure 1. The vibrational spectra corresponding to the four tautomers, PED analysis, and isotopic shifts are given in Tables S2−S5 of the Supporting Information. We predicted that resonance Raman spectroscopy in combination with DFT calculations would allow reliable discrimination between these tautomers through the C8═O stretch mode and the intense ring modes of purines.

The spectra of 8-oxoguanosine and 7-allyl-8-oxoguanosine in Figure 4A,C are similar. The spectrum of GMP (Figure 4E), on the other hand, has a very different intensity pattern. As shown in Figure 1, 7-allyl-8-oxoguanosine is a model com-

TABLE 2: Experimental (FTIR and Raman) and Computed[a] IR and Raman Wavenumbers[b] of 8-Oxoguanosine (8-oxodG), 7-Allyl-8-oxoguanosine (7AOG), and GMP in Water

8-oxodG FTIR	8-oxodG Raman	7AOG FTIR	7AOG Raman	8-oxodG DFT	assignment	PED (%)[c]	guanine Raman	guanine DFT	assignment	PED (%)[c]
1705	1715	1704	1706	1871	C8O str, N7H be	CO str (72), NC str (−11)				
1681	1677	1676	1674	1817	C6O str, N1H be, C5C6 str	CO str (−62), CC str (20)	1681	1830	C6O str, N1H be, C5C6 str	CO str (73), CNC be (−10)
1637		1645		1667	NH_2 sci, N2C2 str, N1C6 str, C4C5 str	HNH be (51), NC str (−14), NC str (14)		1677	NH_2 sci, N1H be, C2N3 str, N1C6 str	HNH be (39), NC str (−22), NC str (17)
		1627			allyl					
1594	1601	1596		1616	C4C5 str, N1C2 str, N3C4 str, NH_2 sci, N9H str	NC str (28), NC str (−11), HNH be (17)	1576	1623	NH_2 sci, C2N3 str, C4C5 str, N9H be, N7C8 str	HNH be (−30), NC str (−17)
	1610		1605	1644	NH_2 sci, C5C6 str, C2N3 str, N1C6 str, C5N7 str	CC str (−37), NC str (16)	1602	1632	NH_2 sci, N3C4 str, N9H be, C2N3 str, N7C8 str	NC str (−13), NC str (18), NC str (−10), HNC be (−10), HNH be (10)
1525	1534	1512	1525	1563	N2C2 str, NH_2 sci, C4N9 str, N7C8 str N1C2 str, C5C6 str, N1H be	NC str (−14), NC str (10), HNC be (−12), HNH be(10)	1537	1570	N2C2 str C4N9 str, N7C8 str N1C2 str, N1H be, NH_2 sci, C8H be	NC str (−16), CNC be (−11)
		1532			allyl					
1483					deoxyribose					
1443	1455	1449	1455	1481	N1C2 str, C4N9 str, N1H be, N7H be, C4C5 be	NC str (24), HNC be (12)	1486	1523	N7C8 str, N1C3 str, N3C4 str, C8H be, N1H be	NC str (41), HCN be (−10)
1424	1445	1426	1433	1472	N7H be, C5N7 str, C4N9 str	NC str (29), NC str (28), HNC be (−13)	1412	1451	C4C5 str, N1C2 str, N7C8 str, NH_2 rock, N1H be	CNC be (23), NC str (−22), NC str (−13)
							1366	1418	N9H be, C8N9 str, N3C4 str, N7C5 str	HNC be (41), NC str (−24)
							1332	1368	C5N7 str, C4N9 str, C5C6 be, C8H be	NC str (25), CNC str (−13) NC str (10)
		1412			allyl					
		1402			allyl					
1394		1389	1398		deoxyribose					
1352		1367			deoxyribose					
1336	1322	1345		1346	N1H be, N7H be, N3C4 str, N7C8 str, C8N9 str, NH_2 be	HNC be (20), NC str (17), HNC be (10)				
1301		1313	1313	1326	N1H be, N7H be, N7C8 str, C2N2 str	HNC be (26), HNC be (−20), NC str (12)	1204	1307	C8H be, N1H be, C2N2 str, N7C8 be	HNC be (36), NC str (16)
							1319	1338	N1H be, C5N7 str, NH_{2a} be, C2N3 be	HNC be (42), NC str (−12)
1231	1231		1272	1289	N9H be, C8N9 str, N7H be, C5C6 str, N1C6 str, N1H be	HNC be (33), CNC be (14)				
1266		1262		1279	N9H be, N7H be, N3C4 str, C5C6 str, N1H be, C2N2 str	HNC be (23), NC str (−11), HNC be (−10)				
1243		1238	1239		deoxyribose		1240		ribose	
1205		1215			deoxyribose					
	1192	1196	1201	1170	N7H be, N7C8 str, N9H be, N1C6 str, C4N9 be	NC str (18), NC str (−17), NCC be (11)	1040	1174	C8H be, N9H be, C4N9 str, C5N7 be	HCN be (24), CNC be (−13)
							1173	1159	NH_2 rock, N1C6 str, C2N3str	HNC be (38), NC str (−15)
1149	1144	1160	1161	1122	NH_2 rock, N1C6 str, C4N9 str, C2N3 str, N9H be	NCN be (29), NC str (19)	1111	1092	N9C8 str, N9H be, C8H be	NC str (42), HNC be (28), HCN be (−10)
1106		1128			deoxyribose					
1119		1116			deoxyribose					
1052	1073	1063	1084	1060	N1C6 str, NH2 be, N7C8 str, C8O be, C8N9 str	HNC be (21), CNC be (−19), CCN be (18)	1079	1085	N1C6 be, NH_2 rock, N3C4 str, C4N9 str, N9H be	NC str (38), OCN be (−16), HNC be (15)
		1095	1099		allyl					
		1078			allyl					
1018	1015	1016	1015	1040	N1C2 str, C2N3 str, N1H be, NH_2 rock, N9H be, C4N9 str, N7H be	NC str (38), HNC be (−12), HNC be (11)	1015	1048	C2N2 str, N1C2 str, C2N3 str, N1H be	NC str (38), NC str (13)
		1045			deoxyribose					

TABLE 2: Continued

8-oxodG FTIR	8-oxodG Raman	7AOG FTIR	7AOG Raman	8-oxodG DFT	assignment	PED (%)[c]	guanine Raman	guanine DFT	assignment	PED (%)[c]
991	977	980	977	975	C8N7 str, N7C8 str, N8H be	NCC be (42), NCC be (19), CNC be (−11)	1020	956	N7C8N9 str	NCN be (56), NC str (10)
968					deoxyribose					
945	923	937			deoxyribose					
915		924			deoxyribose					
							868	836	C2N3C4 rock, C5N7 str, C8H be, NH_{2a} be	CNC be (25), NCN be (16), NC be (12), NCC be (11), CNC be (−10)
894	892	894	895	873	C5N7 str, N7H be, C4C5 be, N3C4 str, N1C6 str	NCN be (25), CC str (11), NC str (11)				
856		867			deoxyribose					
								815	C8H be (out)	HCNC tors (80)
							789	774	C4C5C6 be, C8H be	ONCC tors (−33), CNCN tors (−25), NNCC out (−19)
		822	820		allyl					
792	785	791	744	767	N9H be, C2N2 str, N7H be, N1C6 str	CNC be (30), CNC be (−14)				
764		752			deoxyribose					
		765		749	C2N3C4 be (out), C8O be	ONNC out (−60), NNNC out (−10)				
733		725	723	736	N3C4C5 be (out), C6N1C2 be (out), N7C8 be	NNNC out (22), ONCC out (−20), ONCC out (−17), NCNC tors (13)				
		716			allyl					
701		700			deoxyribose					
								732	N2C2N3 be (out), N1H be	NNNC out (50), ONCC out (21), NCNC tors (16)
681		678	680	709	N1H be, C6O str	ONCC out (48), NNNC out (26)	821	700	N1H be, C4C5 be, N1C2 be, C6O be	ONCC out (−28), NNNC out (22), CNCN tors (11)
642		650		656	NH_2 rock, N9H be, N7H be, C6O be	OCN be (13), NCN be (11), CCN be (10)				
617	625	631	638	676	N1H be, NH_2 sci, N2C2 str, C4N9 str, N9H be, N7H be	NNCC out (19), HNCN tors (18), ONCC out (−12), NNNC out (10)	689	674	C4N9 be, C6O be, NH_2 rock, N1H be	OCN be (17), NCN be (16)
								666	N9H be (out), C8H be (out)	CNCN tors (32), HNCN tors (−20), CNCN tors (−15), HCNC tors (12)
		621			allyl					
605		611	613	610	N1H be (out), in plane ring modes	CCN be (15), CC str (−10)				
586		594		594	N1H be, C5C6 str, NH_2 rock, C4N9 str	HNCN tors (−62)				
				562	NH_2 rock (out), N9H be, N7H be	NCC be (31), OCN be (−16)				
				556	NH_2 be	HNCN tors (68), HNCN tors (−12)				
				502	N9H be, N7H be (out)	HNCC tors (55), HNCC tors (−20)				
							671	627	ring breathing, C6O str, N1C6 str, N1C2 str	CNC be (16), NC str (15), NC str (11), NC str (11)

[a] B3LYP/6-31G**-predicted vibrational spectra. [b] Wavenumbers given in cm^{-1}. Abbreviations: str, bond stretching; be, bending; rock, rocking; sci, scissoring; out, out of plane; tors, torsion. [c] Potential energy distributions (PEDs) calculated using the VEDA 4.0 program.[23]

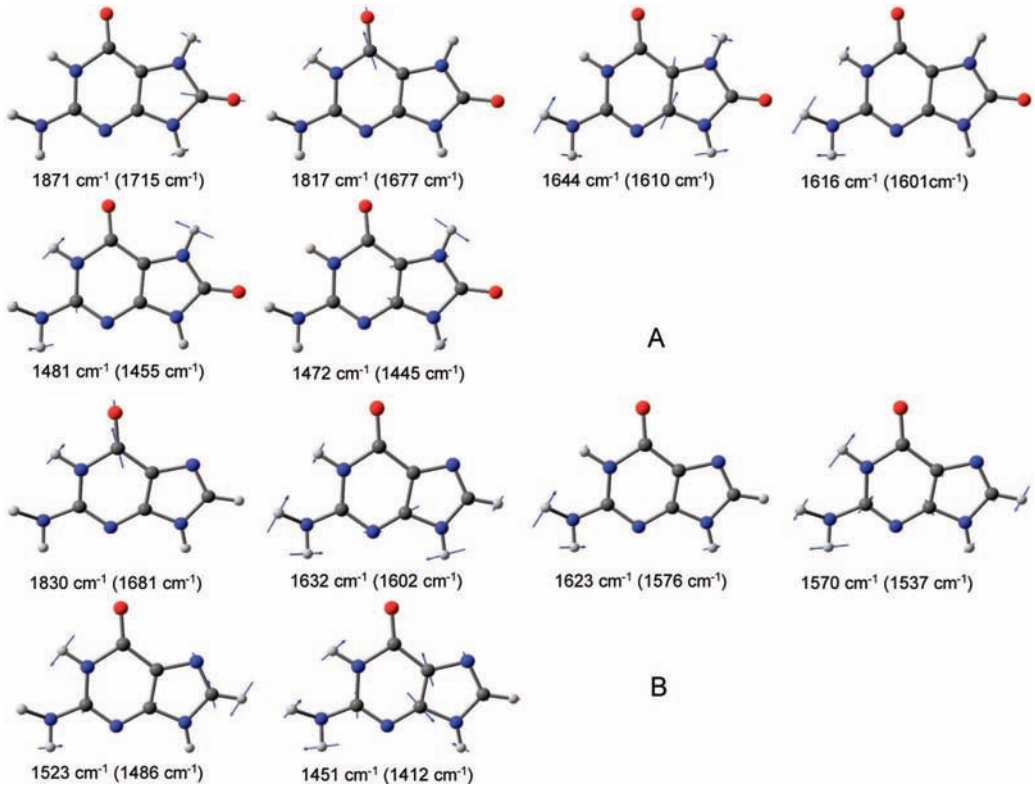

Figure 6. Normal-mode descriptions of selected bands observed in the resonance Raman spectra of (A) 8-oxoguanine and (B) guanine.

pound, similar to 8-oxoguanosine, but one that can exist only in the C8-ketone form. The tautomerization to the 8-hydroxyenol form that is possible in 8-oxoguanosine is impossible in 7AOG because of the presence of the allyl group at N7. The similarity of the spectra of 8-oxoguanosine and 7-allyl-8-oxoguanosine confirms that 8-oxoguanosine exists in the diketone form in aqueous solution. This is consistent with both the previously reported NMR experiments[13] and ab initio and DFT results.[1,15,16]

The Raman spectra of guanosine-5′-monophosphate in H_2O (Figure 4E) and D_2O (Figure 4F) were obtained with excitation at 260 nm in resonance with the nucleobase. The vibrational spectra and structure of guanine have been extensively studied in the literature using both experimental and theoretical methods. The resonance Raman spectra shown in Figures 4 and 5 are in excellent agreement with the spectra of GMP reported by several groups.[24,27,36,37] Computed vibrational spectra of guanine were compared with those reported by Giese and McNaughton[27] and found to match the trends, as expected given that both calculations used DFT methods. Although previous studies reported assignments of observed spectra with the help of isotope shifts[24,36] or DFT[27] calculations, the correspondence between the computational mode description and experimentally observed isotope shifts was not done in detail. We found that the DFT functional used in this work reproduced isotope effects on the frequencies well, indicating that the computed normal-mode composition is reliable.

The spectrum of 8-oxoguanosine has an intensity pattern distinct from that of GMP, with its most intense band at 1601 cm^{-1}. The spectrum of 8-oxoguanosine obtained with 275-nm excitation contains only one band in the C═O stretching region at neutral pH.[19] The spectrum obtained with 260-nm excitation shown in Figure 4A reveals two C═O stretching modes at 1715 and 1677 cm^{-1}. The band at 1677 cm^{-1} can undoubtedly be assigned to the C6═O stretch of 8-oxoguanosine based on comparison with the C6═O band of GMP (1681 cm^{-1}) and the characteristic broad shape and low relative intensity. The spectrum of 8-oxoguanosine in D_2O shows this band downshifted by 17 cm^{-1}, revealing a coupling of this mode to the N1—H bend. Similar coupling is observed in guanosine.[24] The C8═O stretching mode is predicted at an upshift of 54 cm^{-1} from C6═O by DFT calculations (Table 2); hence, the broad band at 1715 cm^{-1} is assigned to this mode of 8-oxoguanosine. The C8═O stretch is also coupled to an N7—H bending mode, as seen from the vibrational mode diagram in Figure 6. DFT underestimates the coupling of this mode and predicts a lower shift (5 cm^{-1}) than observed in experiments (11 cm^{-1}). The C═O stretching modes in the spectrum of 7-allyl-8-oxoguanosine are observed at 1674 and 1706 cm^{-1} for C6═O and C8═O, respectively. As in the case of 8-oxoguanosine and GMP, the effect of deuterium labeling on the C═O wavenumber indicates that this mode is coupled to the N—H modes. The observed modes of 7-allyl-8oxoguanosine are compared and correlated with the corresponding modes of 8-oxoguanosine in Table 2.

The high-intensity band at ∼1600 cm^{-1} can be deconvolved into two components: 1601 and 1610 cm^{-1}. The presence of two bands in this region is corroborated by the spectrum in D_2O, where the band at 1601 cm^{-1} shifts to 1556 cm^{-1}. DFT calculations predict three ring modes at 1667, 1644, and 1616 cm^{-1}, all of which are coupled to NH_2 vibration. The observed experimental modes at 1610 and 1601 cm^{-1} and the computed modes at 1644 and 1616 cm^{-1} couple the pyrimidine and imidazole rings through their common double-bond C4═C5 stretch. Calculations predict a band at 1667 cm^{-1} (IR intensity of 9.4 D^2 amu^2), which is not observed in the Raman spectrum, analogously to the case in guanine, but appears at 1637 cm^{-1} in the IR spectrum (Figure 7). The band at 1534 cm^{-1} is assigned to the N2—C2 stretch. This mode also involves bending vibration of the NH_2 and N1—H groups, although to a lesser extent than in the higher-wavenumber modes discussed above.

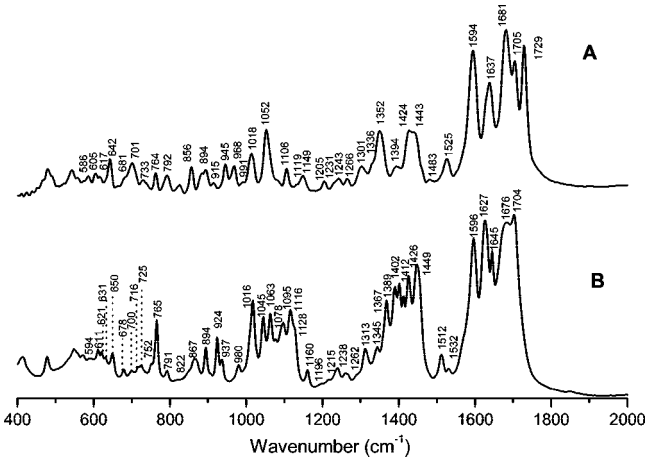

Figure 7. FTIR spectra of (A) 8-oxoguanosine and (B) 7-allyl-8-oxoguanosine in KBr pellet.

The Raman spectra of purines typically contain an intense ring mode at ~1480 cm^{-1} that corresponds to a ring stretching vibration. The Raman spectrum of GMP is dominated by an intense band at 1486 cm^{-1} corresponding to ring stretching vibration in addition to N1—H stretch. The corresponding mode in hypoxanthine appears at 1464 cm^{-1}. In 8-oxoguanosine, however, this mode is at 1455 cm^{-1}, close to that in the N7—H tautomer of hypoxanthine.[38,39] The mode involves vibration of both of the rings and couples to C8—H in guanosine. The computed normal mode for this wavenumber shows the C8—X stretch decoupled from the ring in 8-oxoguanosine. This can be attributed to the more rigid carbonyl group that is now present at C8 in 8-oxoguanosine versus a C—H group in guanosine. The mode at 1445 cm^{-1} in 8-oxoguanosine is centered on the imidazole ring coupled with bending of N7—H. The coupling of these modes to N1—H, N7—H, and NH_2 predicted by DFT calculations is corroborated by the shifts observed in the spectrum upon H/D exchange.

The spectrum of 7-allyl-8-oxoguanosine corresponds to that of 8-oxoguanosine with an overall shift of the spectrum to lower wavenumbers for most modes. The presence of a bulky group at N7 depresses the frequencies of imidazole ring vibrations. Spectra of the three molecules in water and D_2O in the low-frequency region are shown in Figure 5. As in the high-wavenumber region (Figure 4), the spectra of 8-oxoguanosine and 7-allyl-8-oxoguanosine are similar, with additional bands attributable to the presence of the allyl group in the latter spectrum. There is a high-intensity band at 1073 cm^{-1} in 8-oxoguanosine arising from NHC bending. This mode can be used as a marker for protein—nucleobase interactions involving the NH_2 group. Assignments of the remaining bands of the spectra are summarized in Tables 2 and 3.

Solid 8-Oxoguanosine Is Also a Diketone Tautomer. The FTIR spectra of 8-oxoguanosine and 7-allyl-8-oxoguanosine were obtained with powdered samples made into pellets with KBr. The C—O stretch modes are expected to have higher intensity in the IR spectra and to appear at 1705 and 1681 cm^{-1}, close to the positions in the Raman spectrum obtained from solution (Figure 7). The corresponding modes of 7-allyl-8-oxoguanosine are at 1704 and 1676 cm^{-1}. The low-wavenumber NH_2 rocking mode observed at 1073 cm^{-1} in the Raman spectrum of 8-oxoguanosine is also an intense mode in the IR spectrum at 1052 cm^{-1}. Vibrational markers of the allyl group are present at 1627, 1532, 1412, and 1402 cm^{-1} in the high-wavenumber region. The similarity in the spectra of the two compounds confirms that 8-oxoguanosine is in the diketone form in the solid state as well. The detailed assignments of all observed bands are listed in Table 2.

8-Oxoguanosine Incorporated into a DNA Oligomer. The distinct spectrum of 8-oxoguanine as compared to those of guanine and other nucleobases discussed above indicates that it should be possible to distinguish the vibrations of this base when incorporated into an oligomer. The UVRR spectra of 15-base DNA oligomers containing either 8-oxoguanosine [8OG-ssDNA (single-stranded DNA)] or unmodified guanosine (G-ssDNA) at the eighth position are shown in Figure 8. The two spectra are dominated by bands from the unmodified bases: cytosine, thymine, and guanine. The bands arising from the presence of 8-oxoguanosine are masked in the 8OG-ssDNA spectrum. The difference spectrum (Figure 8C) reveals the contribution of the 8-oxoguanosine nucleoside. Bands at 1715, 1608, and 1446 cm^{-1} can be immediately identified from comparison with the spectrum of 8-oxoguanosine in Figure 4A. The band at 1608 cm^{-1} corresponds to the normal-mode vibration from the pyrimidine ring and its peripheral group NH2, and the band at 1446 cm^{-1} is a marker of imidazole ring vibrations involving N7H. Thus, the difference spectra of the oligomers are highly informative of the structure of the incorporated DNA lesion. Although only one carbonyl band of the incorporated 8-oxoguanosine base is observable, the position is unchanged with respect to that in 8-oxoguanosine. This along with the fact that the other vibrational bands are also at similar positions indicates that the 8-oxoguanosine base when incorporated into an oligomer is in a diketone tautomeric form.

Spectra of 8-Oxoguanosine, 7-Allyl-8-oxoguanosine, and GMP in Water and D_2O at High pH. The spectra at neutral pH unequivocally indicate the presence of a single tautomer in both solution and the solid state. If the neutral enol tautomer of 8-oxoguanosine is present at very low concentrations at pH 7.5, it is possible to shift the equilibrium toward the monoenol form by increasing the pH. We examined the spectra of 8-oxoguanosine at increasing pH in the range of 7—12.5. The spectrum at pH 9.5 is shown in Figure 9. A comparison with the spectrum of the GMP anion at pH 11.0 shows a similar Raman intensity profile. GMP can form either a C6—OH enol form or an anion through deprotonation at N1. The absence of the C—O stretching mode in the spectrum of GMP at pH 11.5 (Figure 9C) is consistent with both possibilities. Vibrational spectra predicted using DFT calculations are in agreement with the formation of GMP anion through loss of the H1 proton of the nucleobase.

The spectra of 8-oxoguanosine and 7-allyl-8-oxoguanosine contain a band attributable to a C—O stretch. The band at 1694 cm^{-1} in the 8-oxoguanosine is assigned to the C8—O stretch of the imidazole ring, following the prediction of DFT calculations and by comparison with GMP anion (Table 4). Although there is a single band in this region in water, the spectrum of 8-oxoguanine in D_2O reveals the presence of an additional band that can be assigned to the carbonyl stretch (C6—O) of the pyrimidine ring substituent.

In both the neutral enol tautomer and the anion forms of 8-oxoguanosine, one of the C—O stretching modes is expected to downshift significantly. In the spectrum of GMP anion (Figure 9C), the C6—O mode shifts to 1593 from 1681 cm^{-1} in neutral GMP. Close scrutiny of these spectra also shows that the intensity profiles of the observed bands in 8-oxoguanosine, 7-allyl-8-oxoguanosine, and GMP are similar for the lower-wavenumber bands. This suggests that the three bases are in the same protonation state at the indicated pH. At high pH, 7-allyl-8-oxoguanosine can form either the C6—OH enol tautomer or an anion through loss of a proton (H1). 8-Oxogua-

TABLE 3: Experimental and Computed[a] IR and Raman Wavenumbers[b] of 8-Oxoguanosine (8-oxodG), 7-Allyl-8-oxoguanosine (7AOG), and GMP in D_2O

8-oxodG Raman	7AOG Raman	8-oxodG DFT	assignment	PED (%)[c]	guanine Raman	guanine DFT	assignment	PED (%)[c]
1704	1700	1866	C8O str	OC str (74), NC str (−11)				
1660	1660	1809	C6O str, C5C6 str	OC str (−65), CC str (21)	1663	1823	C6O str, N1H be, C5C6 str	OC str (75), CNC be (−11)
		1640	C4C5 be, N9H be	CC str (−40), NC str (18)				
1561	1560	1236	NH_2 sci, N1C6 str, N1H be, N9H be, N7C8 str, C4N9 str, N3C4 str	DND be (32), HNC be (−13), NC str (11)				
1602	1602	1611	C2N3 be, N1C2 be, C6O be, C6N1 str, C5N7 str, C4C5 be	NC str (43), NC str (−11), NC str (−10)	1569	1630	C2N3 str, N3C4 str, N1C6 str, N9H be, N7C5 str, C8H be	NC str (−23), NC str (19), NC str (−10)
					1580	1625	C2N3 str, N9H be, C5C6 str,	NC str (37)
	1541		allyl					
1527	1527	1555	C4C5 str, N1C2 str, C2N2 str, C4N9 str, N1H be, NH_2 sci	NC str (21), NC str (19)	1538	1564	C8H be, N2C2 str C4N9 str, N7C8 str	NC str (22), CNC be (17)
					1480	1514	N7C8 str, N1C2 str, N3C4 str, C2N2 str, C8H be	NC str (35), NC str (12), NC str (−10)
1436	1428	1465	C5N7 str, C4N9 str, N9H be, N1C2 str, NH_2 be	NC str (31), NC str (16), NC str (11)	1403	1438	C4C5 str, N1C2 str, N7C8 str, C4C9 str	NC str (−22), NC str (−20), CNC be (20)
1447	1453	1434	N1C2 str, C5N7 str, N7H be	NC str (19), NC str (−19), NC str (11), CC str (−10)	1358	1418	N9H be, C8N9 str, N1C2 str, N7C5 str	HNC be (43), NC str (−24)
	1412		allyl					
1273	1262	1292	N9H be, NH_2 sci, N1H be, N3C4 str, C8N9 str, N1C6 str	HNC be (47), NC str (−11), DND be (10)	1270	1244	NH_2 sci, N1H be, N1C6 str, N1C2 str	DND be (48), DNC be (10)
1242	1238	1214	N1C6 str, NH_2 sci, C5C6 str, C5N7 str, N7C8 str, N7H be, C8N9 str, C4N9 str, N9H be	NC str (18), CC str (−14), NC str (−13)	1329	1367	C5N7 str, C4N9 str, C5C6 be, C8H be	NC str (36), CNC be (−13), NC str (10)
1378	1310	1310	C5N7 str, N7C8 str, C8N9 str	NC str (27), CNC be (−12), NCC be (−12), OCN be (10)	1317	1314	C8H be, C5N7 str, N7C8 be, C2N3 str, N3C4 str	HCN be (35), NC str (20), NC str (−11), CNC be (10)
1015	1015	1044	N7H be, N1C6 str, C2N3 str, C5N7 str, C8N9 str	DNC be (16), NCN be (−13), NC str (−12)				
	1161		allyl					
1184	1189	1082	NH_2 sci, C2N2 str, C8N9 str, N7H be, N9H be	NC str (−14), DND be (−14), DNC be (12), NC str (11), HNC be (−10)	883	1090	N9C8 str, N9H be, C8H be	NC str (44), HNC be (31), HCN be (−12)
					984	1077	NH_2 sci, N1H be, N1C2 str, C6O be, N9C4 str	OCN be (−16), DND be (−15), NC str (13), DNC be (12)
					1045	1179	C8H be, N9H be, C4N9 str, C5N7 be	HCN be (−24), CNC be (12)
	1116		allyl					
1136	1076	1126	N1C6 str, N1H be, NH_2 sci, C2N2 str, N7C8 str, N9H be	DND be (−14), CNC be (−12), DNC be (−11)	1168	1133	NH_2 sci, N1C6 str, C2N3str, N1H be	NC str (37)
984	987	960	N1H be, NH_2 rock, N1C6 str, N1C2 str, C8N9 str	NCC be (20), DNC be (18), DNC be (11)	1114	978	NH_2 rock, N1H be, N7C6 str, C2N3 str	NCN be (−16), DNC be (14), DNC be (12)
	933		allyl					
870	844	919	N1C6 str, N1H be, N7H be, NH_2 rock	NCC be (22), CC str (12), DNCC be (−12)	1029	948	N7C8N9 str, NH_2 rock, N1H be, N1C6 str	NCN be (39)
821	805	858	N1H be, NH_2 rock, N7H be, N1C2 str	DNC be (31), DNC be (−24), NC str (−13)	1015	877	N1H be, NH_2 rock, N1C2 str	DNC be (27), DNC be (−18), NC str (17)
						815	C8H be	HCNC tors (81)
		793	N7H be, N1H be, NH_2 rock, C5N7 str	DNC (23), NCN be (12)	843	805	N1H be, N_2H_2 rock, N_3C_4 str, C_5N_7 str	CNC be (19), DNC be (−13), NC str (11), NCN be (11)
					690	774	C8H be, C5N7 str, C4C5 be, N1C6 str, C5C6 str	ONCC out (33), CNCN tors (26), NNCC out (19)
779	768	751	N9H be, NH_{2a} be, N1C6 str, N1H be, N1C2 str, C4N9 str	CNC be (21), CNC be (−10)				
					800	719	C2N3 str, C2N2 be (out), NH_2 rock	NNNC out (56), ONCC out (16), NCNC tors (15)
	708	746	C8O be (out), N9H be	ONNC out (−66)				
					607	692	C4N9 str, C6O be, N1C6 str, C5N7 str	ONCC out (−38), NNNC out (18), NNCC out (13), CNCN tors (13), CNCN tors (10)
726	726	732	N3C4C5 be (out), C6N1C2 be (out), N7C8 be	ONCC out (−28), NNNC out (17), ONCC out (−15), NCNC tors (13)				
						665	C8H be (out), N9H be (out)	CNCN tors (35), HNCN tors (−23), CNCN tors (−18), HCNC tors (13)
669	688	698	NH_2 rock, N1H be, C6O be	ONCC out (38), NNNC out (38)				
						625	NH_2 rock, N1H be, C4C5 str	CNC be (23), OCN be (−11)

TABLE 3: Continued

8-oxodG Raman	7AOG Raman	8-oxodG DFT	assignment	PED (%)[c]	guanine Raman	guanine DFT	assignment	PED (%)[c]
614	618	667	C5C6 be (out), C1C2 be (out), N1C6 be (out), N9H be	ONCC out (−29), NNCC out (26), NCCN tors (13)				
					673	615	C5C6 str, N1C6 str, N1H be, NH_2 rock, C4N9 str, N1C2 str	NC str (14), NCN be (12), NCC be (−10)
		619	C4C5 str, N3C4 str, N7H be, N9H be, NH_2 be	CCN be (25)				

[a] B3LYP/6-31G**-predicted spectra. [b] Wavenumbers given in cm^{-1}. Abbreviations: str, bond stretching; be, bending; rock, rocking; sci, scissoring; out, out of plane; tors, torsion. [c] Potential energy distributions (PEDs) calculated using the VEDA 4.0 program.[23]

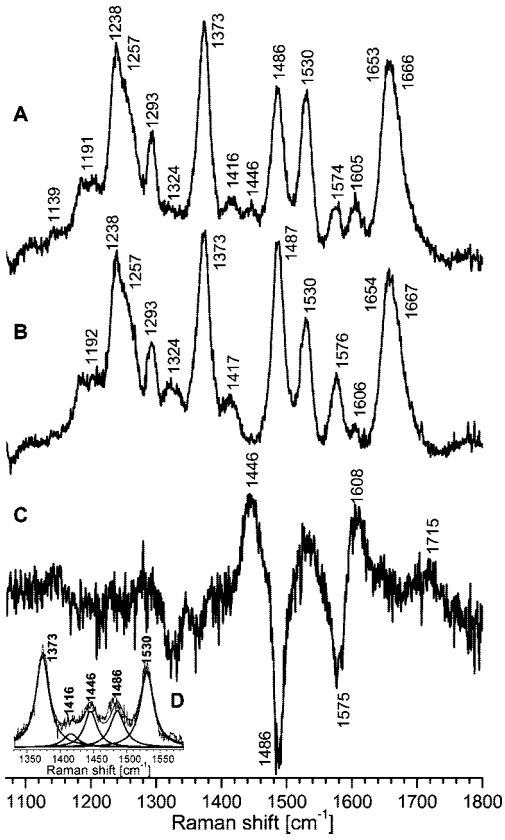

Figure 8. UVRR spectra of ssDNA oligomers: (A) 5′-CTCTCTC(8-oxoguanosine)GCCTTCC-3′, (B) 5′-CTCTCTCGGCCTTCC-3′, (C) difference spectrum (A − B), and (D) inset showing a section of the spectrum with contributions from 8-oxoguanosine.

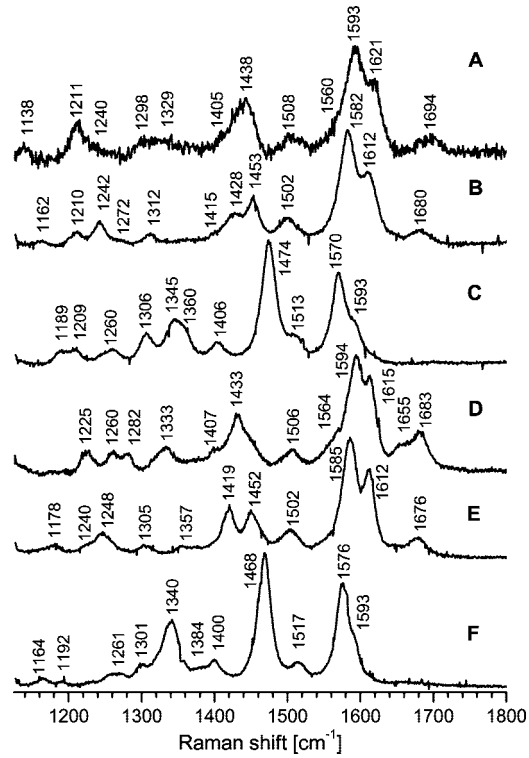

Figure 9. UVRR spectra of (A) 8-oxoguanosine in water at pH 9.5, (B) 7-allyl-8-oxoguanosine in water at pH 11.0, (C) GMP in water at pH 11.5, (D) 8-oxoguanosine in D_2O at pD 9.5, (E) 7-allyl-8-oxoguanosine in D_2O at pD 11, and (F) GMP in D_2O at pD 11.5 recorded with laser excitation at 260 nm.

nosine has the additional possibility of deprotonation at N7. The spectra of both the enolic and anionic species contain a single carbonyl mode, the C8═O stretch. The presence of a single C—O band in the Raman spectra (Figure 9B,E) indicates the presence of a single tautomeric species in solution. We computed the structure and vibrational spectrum of the neutral enolic and anionic forms for guanine and 8-oxoguanine. The computed spectra and experimental data are in agreement with the anionic form and not the neutral enolic form. Further evidence that the observed spectrum corresponds to that of deprotonated 8-oxoguanosine is seen in the spectrum in D_2O. Deuterium labeling differentially shifts the two C═O modes to 1655 and 1683 cm^{-1}, indicating that both carbonyl bonds are still present in 8-oxoguanosine anion, although they are weaker than in the neutral form. The 7-allyl-8-oxoguanosine molecule serves as a model compound to distinguish between the anion with deprotonation at the N7 position versus that with deprotonation at N1 because the deprotonation of 7-allyl-8-oxoguanosine must necessarily occur at N1 position. The correspondence of the spectra of 8-oxoguanosine anion and its 7-allyl-8-oxoguanosine analogue confirms that the N1 proton is lost when the pH is raised.

Previous NMR and computational studies support this conclusion. The UV spectra of 8-oxodG recorded at various pH values show two pK_a values, 8.6 and 11.7,[12] with the first deprotonation at the N1 position. This conclusion was based on comparison of the UV spectra of 8-oxodG and its other derivatives, 1-methyl-8-oxoguanosine and 7-methyl-8-oxoguanosine.[27] The absorption spectra of 8-oxodG and 7-methyl-8-oxoguanosine at pH 8.8 showed similar wavelength maxima, indicating that both molecules undergo ionization at the N1 position.[12] ^{13}C and ^{15}N NMR experiments indicate the formation of a monoanion at pH 9.5, with N1 undergoing ionization, based on chemical shifts observed at the C6, C2, and N1 positions of 8-oxodG.[12,40] Finally, high-level DFT calculations in combination with a Poisson−Boltzmann continuum solvation model confirm that high pH does not shift the equilibrium toward the enol form and that the deprotonation site corresponding to the first pK_a is N1.[1]

TABLE 4: Experimental (Raman) and Computed[a] IR and Raman Wavenumbers[b] of 8-Oxoguanosine Anion (8-oxodG) at pH 9.5 and 7-Allyl-8-oxoguanosine Anion (7AOG) at pH 11.0 in Water and D_2O

8-oxodG in water	8-oxodG[d] DFT	7AOG in water	assignment	PED (%)[c]	8-oxodG in D_2O	8-oxodG[d] DFT	7AOG in D_2O	assignment	PED (%)[c]
1694	1814	1680	C8O str, N7H be	OC str (70), NCN be (15)	1683	1808	1676	C8O str	OC str (72), NCN be (14)
	1712		C6O str, C4C5 str	OC str (52), CC str (16), CNC be (−13)	1655	1711		C6O str	OC str (55), CC str (15), CNC be (−10)
1621	1669	1612	C4C5 str, C4N9 str, N3C4 str, N1C2 str	CC str (33), OC str (−17), NC str (−17)	1615	1665	1612	C4C5 str, N3C4 str, N9H be, N1C2 str, C6O str	CC str (−35), NC str (18), OC str (15)
1593	1615	1582	NH_2 sci, C2N2 str	HNH be (67)	1594	1271	1585	N9H be, NH_2 sci, N1C6 str, N2C2 str, N3C4 str, C8N9 str (pyr+Im.ring breathing)[e]	HNC be (42), NC str (11), NC str (−10)
1560	1560		N7H be, C4C5 str, C5C6 str, C2N3 str, NH_{2a} be, C5N7 str, C4N9 str	NCC be (−19), NC str (−18), CCN be (13)	1564	1549		C5C6 str, C4C5 str, N1C2 str, C2N3 str, C4N9 str	NC str (−20), NCC be (−20), CCN be (12)
1508	1485	1502	NH_2 be, N1C2 str, N7H be, C4C5 str	NC str (24), CC str (−23), HNC be (11)	1506	1460	1502	C4C5 str, N1C2 str, C4N9 str	NC str (27), CC str (−25), NC str (15)
		1453	allyl						
1438	1429	1428	N2C2 str, NH_2 sci, N1C6 str, N9H be, C4N9 str	NC str (24), NC str (−21), NC str (−16)	1433	1448	1452	C2N2 str, N1C6 str, C4N9 str, N9H be, NH_2 sci	NC str (34), NC str (−21), NC str (−15)
1405	1414	1415	N7H be, C5N7 str, C4N9 str, C2N3 str, NH_2 rock	HNC be (23), NC str (−23), NCN be (−11)	1407	1370	1419	C5N7 str, N7H be, C4N9 str, N1C6 str, C2N3 str	NC str (21), NCN be (12)
1329	1344	1312	Im,[d] ring breathing, C5N7C8 str, C8O be	NC str (32), CNC be (23), OCN be (−16)	1333	1334	1357	C8O be, N7C8 str, N7H be	NC str (35), CNC be (20), OCN be (−18)
1298	1271	1272	N9H be, N7H be, NH_2 sci, C5C6 str	HNC be (24), HNC be (−19)	1282	1178	1305	NH_2 sci, C4N9 str, N7C8 str, C5C6 str	DND be (23), NC str (11)
1240	1255	1242	N9H be, N7H be, C5C6 str, C2N3 str	HNC be (27), NC str (−19), NC str (10), HNC be (10)	1260	1224	1248	N1C6 str, N9H be, NH_2 sci, C5C6 str	NC str (25), HNC be (14), NC str (−10)
1211	1193	1210	NH_2 rock, N1C6 str, N7H bend	NC str (26), HNC be (26), NC str (−13), NC str (−11)	1225	1128	1240	N1C6 str, NH_2 sci, N9H be, C4N9 str	NC str (22), DND be (18), NC str (−10)
1138	1159	1162	N9H be, N7H be, NH_2 rock	NC str (−18), HNC be (13), NC str (11)		1058	1178	N9H be, N7H be, NH_2 be	DNC be (25), NC str (19), NCC (−12)

[a] B3LYP/6-31G**-predicted spectra. [b] Wavenumbers given in cm^{-1}. Abbreviations: str, bond stretching; be, bending; rock, rocking; sci, scissoring; out, out of plane; tors, torsion. [c] Potential energy distributions (PEDs) calculated using the VEDA 4.0 program.[23] [d] Deprotonated at N1. [e] Im, imidazole; pyr, pyrimidine ring.

The modes corresponding to vibrations of the imidazole and pyrimidine rings in 7-allyl-8-oxoguanosine anion have higher intensity and, therefore, a better signal-to-noise ratio. The band at 1621 cm^{-1} involves the C4—C5 and C4—C9 modes that connect the pyrimidine and imidazole rings. The NH_2 scissors vibration is observed at 1593 cm^{-1} and is coupled to the C2—N2 stretch. The pyrimidine ring mode is observed at 1438 cm^{-1} but moves to 1433 cm^{-1} in D_2O. As expected with the loss of the ring proton, the effects of deuteration on the spectra of the anion are small.

We found that the 6,8-diketone tautomer is the principal species present in neutral solution in both 8-oxoguanosine in water and 8-oxoguanosine incorporated into an oligomer. Reliable assignments of the observed Raman bands were made based on comparison with the unmodified base, H/D exchange, and high-level DFT calculations. A detailed normal-mode analysis was carried out on the neutral and deprotonated forms, which indicated that there are intense modes corresponding to vibrations of the ring substituents that are expected to interact with the protein. These assignments provide the basis for using resonance Raman spectroscopy as a probe of the protein-bound lesions and predicting the modes that will report on the nucleobase—protein interaction.

One of the reported pK_a's of 8-oxoguanine is at 8.6.[12] To determine whether there is a shift in the keto—enol tautomeric equilibrium, the spectrum of 8-oxoguanosine at pH 9.5 was analyzed. DFT calculations on the possible products of deprotonation and enolic forms were reported. Comparison of the experimental and computational results allowed unequivocal assignment of the observed species. Instead of a shift in the tautomeric equilibrium, we found that 8-oxoguanosine undergoes deprotonation at high pH. The preferred site for deprotonation is N1 of the pyrimidine ring.

The binding of glycosylases to 8-oxoguanosine has been proposed to involve lowering of the pK_a of the damaged base. This would result in deprotonation of 8-oxoguanosine, and hence, 8-oxoguanosine would be bound in its anionic form. Knowledge of the likely site for deprotonation provides insight into the mechanism of nucleobase recognition. The experiments reported here clearly demonstrate that 8-oxoguanosine is unlikely to deprotonate at N7, and thus, the H7 proton could probably be used as a major structural marker by enzymes to distinguish 8-oxoguanosine from guanosine.

Conclusions

8-Oxoguanosine and guanosine have similar absorption spectra, are nonfluorescent, and cannot be used to carry out fluorescence-based biophysical studies of the enzyme—substrate complex. We have demonstrated here that the resonance Raman spectra of the nucleobases are highly sensitive to modifications such as oxidation. The spectral markers of ring substituents and their normal-mode descriptions obtained here form the basis for using the vibrational spectra as markers of enzyme—nucleobase interactions. We have shown that 8-oxoguanosine, when incorporated into an oligomer, can be used as a site-specific probe for DNA because of its unique spectrum that is distinct from that of the natural bases. DFT calculations of vibrational spectra reliably reproduce trends in the experimental frequencies. Combined with DFT calculations and a detailed normal-mode analysis, ultraviolet resonance Raman spectroscopy is a powerful tool for investigating DNA—protein interaction in these systems.

Acknowledgment. This research was supported by grants from the National Centre for Biological Sciences (NCBS); Tata Institute of Fundamental Research; and the Department of Biotechnology, India. M.P. was supported by NCBS and the Innovative Young Biotechnologist Award of the Department of Biotechnology, India. N.J. was supported by a Ph.D. fellowship of the Council for Scientific and Industrial Research, India.

Supporting Information Available: Mulliken charges of the energy-minimized structures of guanine, 8-oxoguanine, and 8-hydroxyguanine (Table S1) and vibrational spectra of the keto−enol tautomers of 8-oxoguanine (Tables S2−S5). This information is available free of charge via the Internet at http://pubs.acs.org.

References and Notes

(1) Jang, Y. H.; Goddard, W. A., III; Noyes, K. T.; Sowers, L. C.; Hwang, S.; Chung, D. S. *Chem. Res. Toxicol.* **2002**, *15*, 1023.
(2) Breen, A. P.; Murphy, J. A. *Free Radical Biol. Med.* **1995**, *18*, 1033.
(3) Lindahl, T. *Nature* **1993**, *362*, 709.
(4) Cadet, J.; Bourdat, A. G.; D'Ham, C.; Duarte, V.; Gasparutto, D.; Romieu, A.; Ravanat, J. L. *Mutat. Res./Rev. Mutat. Res.* **2000**, *462*, 121.
(5) Ravanat, J. L.; Cadet, J. *Chem. Res. Toxicol.* **1995**, *8*, 379.
(6) Ohno, M.; Miura, T.; Furuichi, M.; Tominaga, Y.; Tsuchimoto, D.; Sakumi, K.; Nakabeppu, Y. *Genome Res.* **2006**, *16*, 567.
(7) Prat, F.; Houk, K. N.; Foote, C. S. *J. Am. Chem. Soc.* **1998**, *120*, 845.
(8) Helbock, H. J.; Beckman, K. B.; Shigenaga, M. K.; Walter, P. B.; Woodall, A. A.; Yeo, H. C.; Ames, B. N. *Proc. Natl. Acad. Sci. U.S.A.* **1998**, *95*, 288.
(9) Luo, Y. Z.; Henle, E. S.; Linn, S. *J. Biol. Chem.* **1996**, *271*, 21167.
(10) Cheng, K. C.; Cahill, D. S.; Kasai, H.; Nishimura, S.; Loeb, L. A. *J. Biol. Chem.* **1992**, *267*, 166.
(11) Shibutani, S.; Takeshita, M.; Grollman, A. P. *Nature* **1991**, *349*, 431.
(12) Culp, S. J.; Cho, B. P.; Kadlubar, F. F.; Evans, F. E. *Chem. Res. Toxicol.* **1989**, *2*, 416.
(13) Oda, Y.; Uesugi, S.; Ikehara, M.; Nishimura, S.; Kawase, Y.; Ishikawa, H.; Inoue, H.; Ohtsuka, E. *Nucleic Acids Res.* **1991**, *19*, 1407.
(14) Reynisson, J.; Steenken, S. *J. Mol. Struct. (THEOCHEM)* **2005**, *723*, 29.
(15) Cysewski, P. *J. Chem. Soc., Faraday Trans.* **1998**, 3117.
(16) Cysewski, P.; Jeziorek, D. *J. Mol. Struct. (THEOCHEM)* **1998**, *430*, 219.
(17) Kouchakdjian, M. *Biochemistry* **1991**, *30*, 1403.
(18) Uesugi, S.; Ikehara, M. *J. Am. Chem. Soc.* **1977**, *99*, 3250.
(19) Kundu, L. M.; Loppnow, G. R. *Photochem. Photobiol.* **2007**, *83*, 600.
(20) Schmidt, M. W.; Baldridge, K. K.; Boatz, J. A.; Elbert, S. T.; Gordon, M. S.; Jensen, J. H.; Koseki, S.; Matsunaga, N.; Nguyen, K. A.; Su, S. J.; Windus, T. L.; Dupuis, M.; Montgomery, J. A. *J. Comput. Chem.* **1993**, *14*, 1347.
(21) Becke, A. D. *J. Chem. Phys.* **1993**, *98*, 5648.
(22) Lee, C. T.; Yang, W. T.; Parr, R. G. *Phys. Rev. B* **1988**, *37*, 785.
(23) Jamróz, M. H. *Vibrational Energy Distribution Analysis VEDA 4.0*; Warsaw, Poland, 2004.
(24) Toyama, A.; Hanada, N.; Ono, J.; Yoshimitsu, E.; Takeuchi, H. *J. Raman Spectrosc.* **1999**, *30*, 623.
(25) Leszczynski, J. *J. Mol. Struct. (THEOCHEM)* **1994**, *117*, 37.
(26) Kwiatkowski, J. S.; Leszczynski, J. *J. Mol. Struct. (THEOCHEM)* **1990**, *67*, 35.
(27) Giese, B.; McNaughton, D. *Phys. Chem. Chem. Phys.* **2002**, *4*, 5161.
(28) Leszczynski, J. *Int. J. Quantum Chem.* **1992**, 43.
(29) Leszczynski, J. *J. Phys. Chem. A* **1998**, *102*, 2357.
(30) Sponer, J.; Hobza, P. *J. Phys. Chem.* **1994**, *98*, 3161.
(31) Gorb, L.; Leszczynski, J. *J. Am. Chem. Soc.* **1998**, *120*, 5024.
(32) Chandra, A. K.; Nguyen, M. T.; Uchimaru, T.; Zeegers-Huyskens, T. *J. Phys. Chem. A* **1999**, *103*, 8853.
(33) Lipscomb, L. A.; Peek, M. E.; Morningstar, M. L.; Verghis, S. M.; Miller, E. M.; Rich, A.; Essigmann, J. M.; Williams, L. D. *Proc. Natl. Acad. Sci. U.S.A.* **1995**, *92*, 719.
(34) Banerjee, A.; Yang, W.; Karplus, M.; Verdine, G. L. *Nature* **2005**, *434*, 612.
(35) Fromme, J. C.; Verdine, G. L. *Nat. Struct. Biol.* **2002**, *9*, 544.
(36) Toyama, A.; Hamuara, M.; Takeuchi, H. *J. Mol. Struct.* **1996**, *379*, 99.
(37) Bertoluzza, A.; Fini, G.; Tosi, M. R.; Tugnoli, V. *J. Raman Spectrosc.* **1994**, *25*, 709.
(38) Fernandez-Quejo, M.; de la Fuente, A.; Navarro, R. *J. Mol. Struct.* **2005**, *744*, 749.
(39) Shukla, M. K.; Leszczynski, J. *J. Phys. Chem. A* **2003**, *107*, 5538.
(40) Cho, B. P.; Kadlubar, F. F.; Culp, S. J.; Evans, F. E. *Chem. Res. Toxicol.* **1990**, *3*, 445.

JP8071519